

ICPES 2025

40th INTERNATIONAL CONFERENCE ON PRODUCTION ENGINEERING - SERBIA 2025

DOI: 10.46793/ICPES25.422K



University of Nis Faculty of Mechanical Engineering

Nis, Serbia, 18 - 19th September 2025

PRINTED POROUS STRUCTURES

Nikola KOTORČEVIĆ^{1,*}, Fatima ŽIVIĆ¹, Petar TODOROVIĆ¹, Nenad GRUJOVIC¹

Orcid: 0000-0002-5664-9832; Orcid: 0000-0003-2509-187X; Orcid: 0000-0003-3260-1655; Orcid: 0000-0002-8765-2196

¹Faculty of Engineering, University of Kragujevac *Corresponding author: <u>nikola.kotorcevic@uni.kg.ac.rs</u>

Abstract: This paper investigated the influence of FDM 3D printing input parameters and presented short analysis of various parameters on some specific properties of the printed parts. We examined the effect of layer height on dimensional precision of the printed parts made of polylactic acid (PLA). We experimentally tested three different layer heights (0.16 mm, 0.20 mm, 0.24 mm) and their influence on the geometric accuracy, using cross hatch infill pattern at 70% infill density. Simple 3D model of the printed structure was created to evaluate the porosity in printed part, depending on the layer height. Experimental study, as well as the computational model, both indicated that layer height showed significant influence on the dimensional precision of the printed parts. Layer height as input parameter in 3D printing also impact the accuracy of internal infill structures.

Keywords: additive manufacturing, FDM 3D printing, dimensional accuracy, layer height, Dragonfly software model

1. INTRODUCTION

Additive manufacturing (AM) is a process that fabricates parts through the layer-by-layer deposition of material. It is widely used for prototyping and research applications [1], [2]. The advancement of AM has, to some extent, surpassed conventional manufacturing techniques. With further advancements in this technology, it is likely that this trend will continue, driven by AM cost-effectiveness and versatility, which provide a viable alternative to traditional processes such as injection molding and

plastic forming [1]. Unlike subtractive methods, AM builds parts without removing material, reducing waste except for support structures [3]. Parts made by traditional methods often have better mechanical properties than 3D printed ones due to porosity and anisotropy in manufacturing [4]. However, with adequate optimisation and considering the influence of specific input parameters [5], [6], 3D printing has been used across various industries. Several additive manufacturing processes have been widely used, including: Selective Laser Melting (SLM), Laminated Object Manufacturing (LOM), Selective Laser Sintering (SLS), Fused Deposition Modelling (FDM) etc. [6].

In Fused Deposition Modelling (FDM), a thermoplastic polymer filament is fed through an extruder nozzle onto a build platform precisely controlled temperature conditions [7]. The filament is heated to a molten state within the nozzle, forming a viscous material that is precisely deposited onto the preceding layer. The interlayer bonding is achieved through heat transfer, which induces localized melting and fusion between adjacent layers [8]. The final object is constructed through the sequential deposition of material layers [7]. While elevated extrusion temperatures enhance material fluidity and improve interlayer excessive temperatures adhesion, compromise mechanical properties. This occurs due to residual stress accumulation, irregular material deposition, surface imperfections, and reduced interlayer bonding strength [9].

FDM is widely used due to its simplicity, low cost and high speed [4]. This technology finds applications across diverse sectors, including medical, biomedical, electronics, automotive, and aerospace industries [10].

Most commonly used materials in FDM include: polylactic acid (PLA), poly carbonate (PC), acrylonitrile butadiene styrene (ABS), poly-ether-ether-ketone (PEEK) etc. [3].

PLA, a thermoplastic polymer derived from renewable resources (e.g., sugarcane, corn starch), is particularly notable for its ecofriendliness, biodegradability, and excellent melt flow properties [6]. While polymers dominate FDM material usage, advanced composites incorporating metals, ceramics, or hybrid materials can also be processed, expanding the technology's functional scope [11].

2. INFLUENCE OF 3D PRINTING PARAMETERS ON THE PRINTED PART PROPERTIES

The process begins with the creation of a CAD (Computer-Aided Design) model [12]. This model is converted to a Standard Tessellation Language (STL) file [11] and then sliced in software, which provides the input data for the 3D printer. This means the model is divided into layers [1]. The G-code generated by the slicer software defines the movement of the printer head and nozzle [7]. FDM parts consist of multiple layers containing partially bonded rasters and voids [4]. The nozzle diameter in FDM usually ranges between 0,25 and 0,8 mm [12].

The characteristics of the output part - including dimensional accuracy, geometric precision, and mechanical properties - are influenced by process and machine parameters [13] [1]. Key input parameters such as layer resolution, build orientation, raster angle, temperature, and air gap significantly affect the part's mechanical properties [7].

Layer resolution refers to the thickness of a single layer deposited during one nozzle pass. It directly affects the staircasing effect. Higher layer resolution corresponds to smaller layer thickness values, which can improve surface finish but increase printing time. Studies show that increased layer thickness may reduce load-bearing capacity [7].

Build orientation defines the placement side of the part on the build platform, indicating the object's angular position relative to the platform's horizontal axis. This parameter affects layer arrangement and print quality, as the mechanical properties depend on interlayer fusion quality [7].

Raster angle determines filament alignment within a single layer and directly influences stress distribution under load [7].

Air gap refers to the distance between neighboring rasters [7].

Among the key slicing process parameters, the most significant are: infill density, number

of contours (walls), raster angle, raster pattern, and number of shells [1].

Infill density indicates the percentage of a layer's area that is filled with material relative to the total layer area [1]. Number of contours refers to the count of perimeter boundaries surrounding each layer [1].

Raster pattern determines the nozzle's specific deposition path during printing, which creates the part's internal structure [1].

Number of shells specifies the quantity of bottom and top surface layers covering the part [1].

Experimental studies and analytical models are typically used to predict the geometric quality of FDM-printed parts, though recent efforts have explored reverse CAD approaches [1], [14].

Numerous research studies have investigated the influence of printing parameters on the mechanical behavior of printed parts using various optimization techniques and design of experiment (DOE) methods [2], [3], [4], [5], [6], [11], [15], [16], [17].

The mechanical properties of printed parts are determined by void density, inter-fiber bond strength, and the material properties of the filament [4]. Consequently, printing and process parameters directly affect the quality of bonding between adjacent filaments [4]. Research indicates that parts printed with lower layer heights exhibit higher yield stress and increased elastic modulus [4], [5]. It was also observed that these parts had reduced void density [4].

Printing parameters such as infill percentage, geometric pattern, and layer height play an important role in 3D printing for producing defect-free parts with enhanced mechanical strength [9].

Table 2 presents the effects of key printing parameters on part behavior.

Research indicates that increasing infill percentage enhances tensile strength by reducing voids and improving stress distribution [9].

While higher infill density improves part strength, it also increases object weight. The infill pattern further influences FDM part performance [3]. However, we should keep in mind that higher infill density and lower layer height require longer printing time and higher material cost [3].

Other research shows that infill density and print speed have the greatest effect on flexural, compression, and tensile strength, followed by layer thickness [18].

Giri et al. indicate that increasing the number of contours improves tensile strength, while decreasing layer thickness and air gap enhances surface roughness [20].

Different infill patterns affect the mechanical properties of printed parts. For example, gyroid and honeycomb patterns show similar behavior under bending loads, while the grid pattern demonstrates a smaller increase in bending strength with increasing density [15]. Another study found that in grid and tri-hexagon infill patterns, volume inaccuracy increases with infill density [12].

Table 2. Influence of input parameters on final properties of the printed part

Printing Influenced Printing					
parameter	parameter	Reference			
	Dimensional				
	accuracy,				
	elastic				
	modulus,				
	surface	[1], [2], [7],			
Layer height	roughness,	[18]			
	mechanical	[10]			
	strength				
	(tensile,				
	compression,				
	flexural)				
	Mechanical				
Infill density	strength,	[18], [19]			
mini density	surface	[10], [13]			
	hardness				
Infill nattern	Mechanical	[9], [15]			
Infill pattern	strength	[5], [15]			
Printing temperature	Mechanical				
	strength	[9]			
	(layer fusion)				
	Mechanical				
Raster angle	strength (load	[7]			
	direction)				

It was also proven that maximum hardness is achieved at maximum fill density levels. This occurs because fewer voids in subsurface layers reduce strength [19].

Although voids and spaces often decrease the mechanical strength of parts, FDM remains a valuable technology for creating porous structures. Proper input parameters can produce internal pores, which are required for applications like scaffolds, water filters [21], [22] and separators [23].

3. EXPERIMENTAL SETUP

Using Autodesk Inventor software, we created a 3D model of a syringe nozzle that serves for the positioning of the filter with dimensions of 10 mm diameter and 3.4 mm height, as shown in Figure.

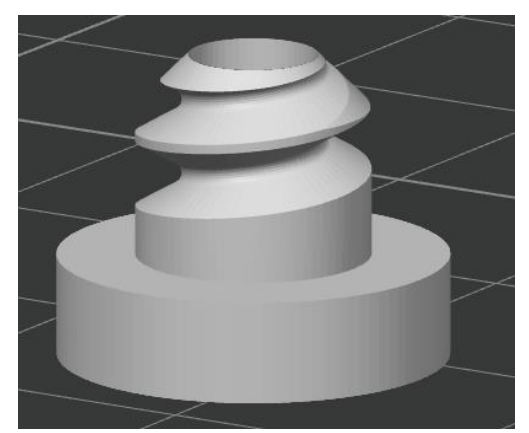


Figure 1. 3D model of syringe filter

In Bambu Studio slicing software, we created three different samples with Cross Hatch infill pattern at 70% infill density. The models contained no top/bottom shells or walls. Layer height was varied between 0.16 mm, 0.20 mm, 0.24 mm as specified in **Table**. Samples were manufactured using a Bambu Lab X1E 3D printer.

Table 2. Sample parameters

Sample	Pattern	Infill [%]	Layer height [mm]
1	Cross		0,16
2	Hatch	70	0,20
3	Пассп		0,24

Each sample was printed five times and measured with a vernier caliper to calculate average values of printed dimensional values. The material was PLA, with nozzle temperature ranging between 190°C and 240°C (automatically adjusted by the machine). All other parameters used default recommended values.

To better analyse subsurface processes, we created a model in Dragonfly software using optical images of each layer. For example: the first sample comprised 21 layers, the second had 17 layers and the third contained 14 layers. We used transparent PLA for the base (layer positioning reference) and red filament for the upper top layer, meaning that all layers were transparent except for the one at the top position (red colour PLA). Under light illumination, only the upper top layer is visible because light can pass through all other transparent layers (Figure 15 and Figure 3).

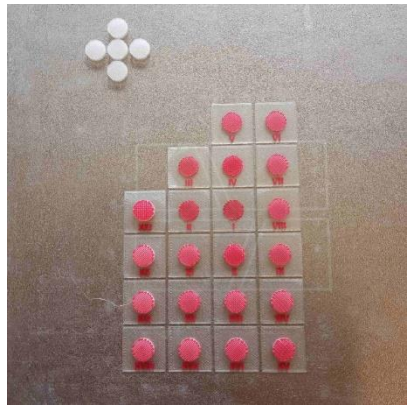


Figure 15. Printing plate; in the top left corner – 5 samples for measuring test with vernier caliper, on the right – layers for Dragonfly model



Figure 3. Layer for Dragonfly model under the light source

We photographed all layers, prepared the images in Photoshop software, and imported

them into Dragonfly software. For example, 21 layer images from Sample 1 were reconstructed into a single 3D model in Dragonfly. Each layer's height was set according to the input layer height parameters specified in Table for each sample.

To evaluate print accuracy, we calculated the percentage error using Formula (1) [24]:

$$\delta = \left| \frac{Dn - D}{Dn} \right| \times 100 \tag{1}$$

where: δ was error percent, Dn represents nominal value (target dimension from ideal model) and D was measured value. The sample with the lowest percent error was considered closest to the ideal model and therefore identified as the optimal result.

4. RESULTS

5.

The measurement results for all samples and their percentage errors (calculated using Formula 1) are presented in **Table**. Since a perfect circle cannot be achieved without wall contours, we considered the smallest measured diameter value. The ideal sample dimensions, as designed in Autodesk Inventor, were: 10 mm in diameter (d) and 3,4 mm in height (H). Any deviation from these values indicates inaccuracies in the printed model due to the selected parameters.

Table 3. Measuring results and percent of error δ

Sample	Average height	δ (H)	Average diameter	δ (d)
Sample	[mm]	[%]	[mm]	(u) [%]
1	3,47	2,1	9,86	1,4
2	3,50	2,8	9,80	2
3	3,50	2,8	9,79	2,1

The results indicate that Sample 1, with the lowest layer height value, achieved the best dimensional accuracy. Samples 2 and 3 showed slightly lower accuracy with their chosen parameters.

In Dragonfly software, we created 3D models by importing optical images of the layers, as demonstrated in Figure .

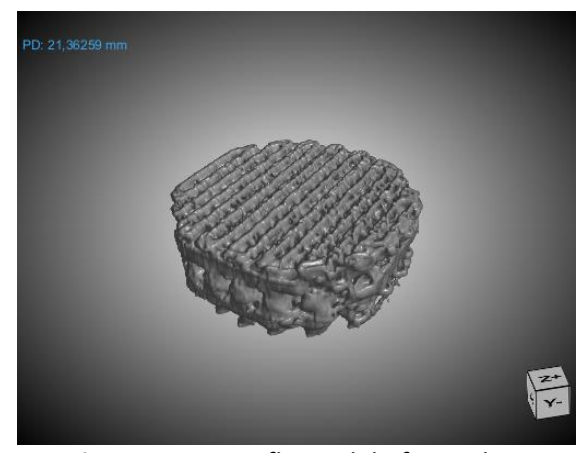


Figure 4. Dragonfly model of Sample 2

The model exhibited inaccuracies compared to the ideal reference sample as designed in CAD. The most significant deviation occurred in diameter dimensions. To determine infill percentage accuracy, we created an ideal reference model with a 10 mm diameter, as shown in **Figure**.

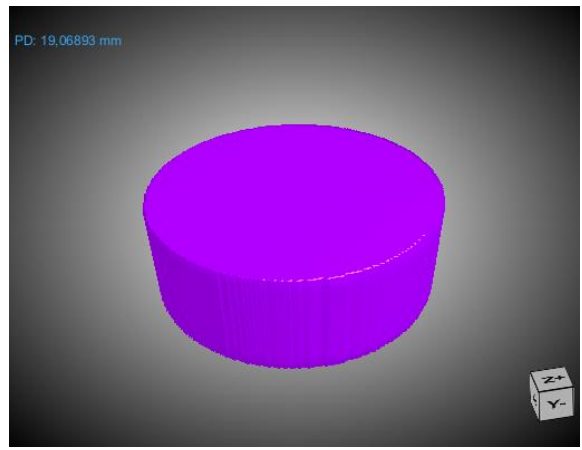


Figure 5. Ideal model

Then, the two regions of interest were considered: volume of pores (Figure) and volume of solid material (filament), as shown in Figure .

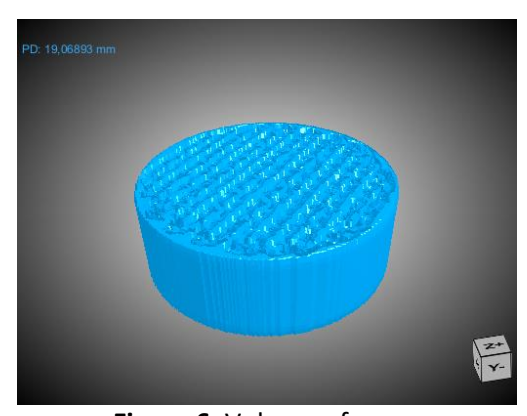


Figure 6. Volume of pores

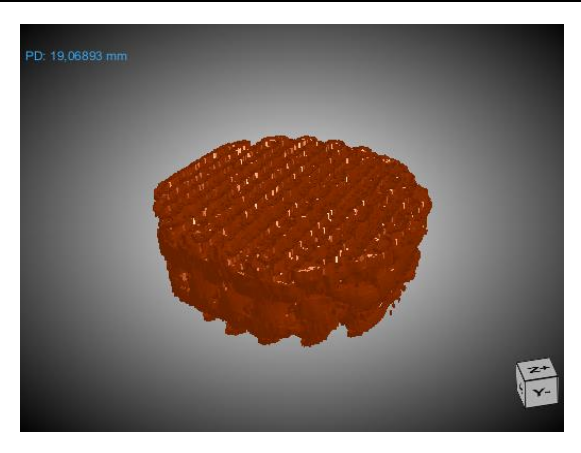


Figure 7. Volume of solid material

The infill percentage was determined by comparing the ideal model's volume with the solid material volume. The nominal value was set at 70% (**Table**). We calculated the error by subtracting the measured filament percentage from this ideal 70% value. The lowest error indicated the optimal print accuracy. All results are presented in

Table

Table 4. Volume percent as provided by the

Dragonfly software and error

Sample	Volume of ideal model [mm³]	Percent of pores [%]	Percent of filament [%]	Error [%]
1	263,8	56	44	26
2	266,7	62	38	32
3	263,8	69	31	39

Because the model does not account for internal material fusion processes or the geometric limitations of filament deposition, the ideal model's volume differed across samples. Sample 2 (17 layers \times 0.2 mm) most closely matched the ideal model's volume, achieving the exact target height of 3.4 mm. Sample 1 (21 layers \times 0.16 mm) and Sample 3 (14 layers \times 0.24 mm) deviated from the target height, resulting in lower volumes. Consequently, we evaluated accuracy solely based on the filament percentage within each printed model, not the ideal dimensions.

The simplified Dragonfly model analysis indicates that Sample 1 achieved the best results, followed by Samples 2 and 3. This suggests that infill accuracy improves with reduced layer height.

In FDM 3D printing, infill percentage refers to how much of the internal volume of a printed part is filled with material, typically using a patterned structure. Porosity, on the other hand, measures the amount of void space (air) within the material or part. There is an inverse correlation between infill percentage and porosity. Higher infill percentage results in lower porosity and vice versa. However, this relationship is not strictly linear, and several factors affect the actual porosity of a part beyond just the infill percentage.

In ideal scenarios (perfect layer adhesion, no gaps, etc.), infill percentage of 70% infill should produce 30% porosity in the final printed part. However, in reality, porosity is usually higher than directly projected by the input infill percentage, due to inter-layer gaps poor fusion, inconsistent extrusion, shell/wall settings and pattern inefficiencies (e.g., some infill types like "grid" vs "gyroid"). 100% infill does not guarantee 0% porosity, due to microscopic voids from imperfect bonding or filament gaps. In reality, a part with 70% infill might have actual porosity closer to 35-40%, especially if the print has only 1-2 perimeters or poorly tuned print parameters.

It can be seen from our experimental results and subsequent software model that porosity was higher than expected 30%, what is in accordance with work of other authors. Therefore, it is important to consider these deviations when designing porous structure for specific applications.

6. CONCLUSION

It can be concluded that higher layer resolution (i.e., lower layer height) improves the geometric precision of printed parts. Additionally, the simplified 3D model analysis of infill percentage showed that samples with

lower layer heights more closely matched the target infill values. This demonstrates that layer height affects not only surface geometry but also internal dimensional accuracy.

ACKNOWLEDGEMENT

This paper is supported through the EIT's Higher Education Initiative SMART-2M, DEEPTECH-2M and A-SIDE projects, coordinated by EIT RawMaterials, funded by the European Union and supported by the Ministry of Education and Ministry of Science, Technological Development and Innovation, Republic of Serbia, Grants: No. 451-03-137/2025-03/200107.

REFERENCES

- [1] B. S. Rupal, K. G. Mostafa, Y. Wang, and A. J. Qureshi, "A Reverse CAD Approach for Estimating Geometric and Mechanical Behavior of FDM Printed Parts," Procedia Manuf., vol. 34, pp. 535–544, 2019, doi: 10.1016/j.promfg.2019.06.217.
- [2] K. S. Patel, D. B. Shah, S. J. Joshi, F. K. Aldawood, and M. Kchaou, "Effect of process parameters on the mechanical performance of FDM printed carbon fiber reinforced PETG," J. Mater. Res. Technol., vol. 30, pp. 8006–8018, May 2024, doi: 10.1016/j.jmrt.2024.05.184.
- [3] N. Lokesh, B. A. Praveena, J. Sudheer Reddy, V. K. Vasu, and S. Vijaykumar, "Evaluation on effect of printing process parameter through Taguchi approach on mechanical properties of 3D printed PLA specimens using FDM at constant printing temperature," Mater. Today Proc., vol. 52, pp. 1288–1293, 2022, doi: 10.1016/j.matpr.2021.11.054.
- [4] S. Garzon-Hernandez, D. Garcia-Gonzalez, A. Jérusalem, and A. Arias, "Design of FDM 3D printed polymers: An experimental-modelling methodology for the prediction of mechanical properties," Mater. Des., vol. 188, p. 108414, Mar. 2020, doi: 10.1016/j.matdes.2019.108414.
- [5] K. Almansoori and S. Pervaiz, "Effect of layer height, print speed and cell geometry on mechanical properties of marble PLA based 3D printed parts," Smart Mater. Manuf., vol.

- 1, p. 100023, 2023, doi: 10.1016/j.smmf.2023.100023.
- [6] S. Sahoo, H. Sutar, P. Senapati, B. Shankar Mohanto, P. Ranjan Dhal, and S. Kumar Baral, "Experimental investigation and optimization of the FDM process using PLA," Mater. Today Proc., vol. 74, pp. 843–847, 2023, doi: 10.1016/j.matpr.2022.11.208.
- [7] S. Khan, K. Joshi, and S. Deshmukh, "A comprehensive review on effect of printing parameters on mechanical properties of FDM printed parts," Mater. Today Proc., vol. 50, pp. 2119–2127, 2022, doi: 10.1016/j.matpr.2021.09.433.
- [8] A. Equbal, A. K. Sood, Md. I. Equbal, I. A. Badruddin, and Z. A. Khan, "RSM based investigation of compressive properties of FDM fabricated part," CIRP J. Manuf. Sci. Technol., vol. 35, pp. 701–714, Nov. 2021, doi: 10.1016/j.cirpj.2021.08.004.
- [9] K. Vijayananth, G. Pudhupalayam Muthukutti, A. Raju, and I. Barsoum, "Integrated optimization and prediction of mechanical properties in FDM printed polyamide/carbon fiber composites using PSI–VIKOR and ANN," Mater., vol. 8, p. 11, 2025, doi: 10.1016/j.nxmate.2025.100932.
- [10] N. A. Fountas, I. Papantoniou, J. D. Kechagias, D. E. Manolakos, and N. M. Vaxevanidis, "Modeling and optimization of flexural properties of FDM-processed PET-G specimens using RSM and GWO algorithm," Eng. Fail. Anal., vol. 138, p. 106340, Aug. 2022, doi: 10.1016/j.engfailanal.2022.106340.
- [11] M. R. Pratheesh Kumar, K. Saravanakumar, C. Arun Kumar, R. Saravanakumar, and B. Abimanyu, "Experimental investigation of the process parameters and print orientation on the dimensional accuracy of fused deposition modelling (FDM) processed carbon fiber reinforced ABS polymer parts," Mater. Today Proc., vol. 98, pp. 166–173, 2024, doi: 10.1016/j.matpr.2023.10.062.
- [12] S. Maurya, B. Malik, P. Sharma, A. Singh, and R. Chalisgaonkar, "Investigation of different parameters of cube printed using PLA by FDM 3D printer," Mater. Today Proc., vol. 64, pp. 1217–1222, 2022, doi: 10.1016/j.matpr.2022.03.700.

- [13] F. Zivic, S. Mitrovic, N. Grujovic, Z. Jovanovic, D. Dzunic, and S. Milenkovic, "The Influence of the 3D Printing Infill and Printing Direction on Friction and Wear of Polylactic Acid (PLA) under Rotational Sliding," J. Frict. Wear, vol. 42, no. 2, pp. 106–111, Mar. 2021, doi: 10.3103/S1068366621020124.
- [14] S. M. Mora, J. C. Gil, and A. M. Camacho López, "Influence of manufacturing parameters in the dimensional characteristics of ABS parts obtained by FDM using reverse engineering techniques," Procedia Manuf., vol. 41, pp. 968–975, 2019, doi: 10.1016/j.promfg.2019.10.022.
- [15] M. M. M. Haque et al., "Impact of process parameters and material selection on the mechanical performance of FDM 3D-Printed components," Hybrid Adv., vol. 10, p. 100502, Sep. 2025, doi: 10.1016/j.hybadv.2025.100502.
- [16] B. Kartikeyan, A. Ponshanmugakumar, G. Saravanan, S. BharathGanesh, and V. Hemamalini, "Experimental and theoretical analysis of FDM AM PLA mechanical properties," Mater. Today Proc., May 2023, doi: 10.1016/j.matpr.2023.05.105.
- [17] L. Kothandaraman and N. K. Balasubramanian, "Optimization of FDM printing parameters for square lattice structures: Improving mechanical characteristics," Mater. Today Proc., Apr. 2024, doi: 10.1016/j.matpr.2024.04.033.
- [18] M. N. Bashir et al., "Investigation of process parameter influence on the mechanical properties of FDM-printed PEEK-carbon fiber composites using RSM and Taguchi methods," J. Mater. Res. Technol., vol. 36, pp. 10199–10209, May 2025, doi: 10.1016/j.jmrt.2025.05.217.
- [19] M. Ramesh and K. Panneerselvam, "Mechanical investigation and optimization of parameter selection for Nylon material processed by FDM," Mater. Today Proc., vol. 46, pp. 9303–9307, 2021, doi: 10.1016/j.matpr.2020.02.697.
- [20] J. Giri, P. Shahane, S. Jachak, R. Chadge, and P. Giri, "Optimization of FDM process parameters for dual extruder 3d printer using Artificial Neural network," Mater. Today

- Proc., vol. 43, pp. 3242–3249, 2021, doi: 10.1016/j.matpr.2021.01.899.
- [21] N. Kotorčević et al., "Material Extrusion 3D Printing of Micro-Porous Copper-Based Structure for Water Filters," Machines, vol. 12, no. 7, p. 470, Jul. 2024, doi: 10.3390/machines12070470.
- [22] N. Fijoł and A. P. Mathew, "Accelerated ageing of 3D printed water purification filters based on PLA reinforced with green nanofibers," Polym. Test., vol. 129, p. 108270, Dec. 2023, doi: 10.1016/j.polymertesting.2023.108270.
- [23] N. Fijoł, A. Aguilar-Sánchez, M.-X. Ruiz-Caldas, J. Redlinger-Pohn, A. Mautner, and A. P. Mathew, "3D printed polylactic acid (PLA) filters reinforced with polysaccharide nanofibers for metal ions capture and microplastics separation from water," Chem. Eng. J., vol. 457, p. 141153, Feb. 2023, doi: 10.1016/j.cej.2022.141153.
- [24] Y. F. Majd, M. S. G. Tsuzuki, and A. Barari, "A Machine Learning Approach to Find Density Percentage Error Resulting by Infill Patterns in Additive Manufacturing," IFAC-Pap., vol. 56, no. 2, pp. 4740–4745, 2023, doi: 10.1016/j.ifacol.2023.10.1236.